Int J Earth Sci (Geol Rundsch) (2009) 98:1365–1380
DOI 10.1007/s00531-008-0321-4

ORIGINAL PAPER

# Precambrian crystalline basement in southern Mongolia as revealed by SHRIMP zircon dating

**Antoine Demoux · Alfred Kröner · Dunyi Liu · Gombosuren Badarch**

Received: 4 December 2007 / Accepted: 19 April 2008 / Published online: 14 May 2008


**Abstract** Single zircon ages determined by ion microprobe (SHRIMP II) for granitoid gneisses from the southern slope of the Baga Bogd massif (Gobi-Altai, southern Mongolia) reveal several episodes of zircon growth, ranging from late Palaeoproterozoic to late Cambrian. The oldest events are documented by a zircon crystallization age for a gneiss protolith at 1519 ± 11 Ma and by a xenocrystic zircon from a dark grey augen-gneiss yielding an age of c. 1701 Ma. Discrete igneous events are recorded in granite-gneisses with protolith emplacement ages of 983 ± 6, 956 ± 3 and 954 ± 8 Ma. These ages provide the first record of early Neoproterozoic magmatic activity in this region. A much younger and discrete magmatic event is recorded by several dioritic to granitic orthogneisses which are tectonically interlayered with the older gneisses and have protolith emplacement ages between 502 and 498 Ma. These late Cambrian granitoids of calc-alkaline affinity are likely to have been emplaced along an active continental margin and suggest that the Baga Bogd Precambrian crustal fragment was either docked against the southward (present-day coordinates) growing margin of the CAOB or was a large enough crustal entity to develop an arc along its margin. We speculate that the Precambrian gneisses of this massif may be part of a crustal fragment rifted off the Tarim Craton.

**Keywords** Central Asian Orogenic Belt · Mongolia · Granitoid gneisses · Zircon · SHRIMP dating

G. Badarch deceased.

A. Demoux (✉) · A. Kröner
Institut für Geowissenschaften, Universität Mainz,
55099 Mainz, Germany
e-mail: demoux@uni-mainz.de

D. Liu
Beijing SHRIMP Center, Institute of Geology,
Chinese Academy of Geological Sciences,
26 Baiwanzhuang Road, 100027 Beijing, China

G. Badarch
Institute of Geology and Mineral Resources,
Mongolian Academy of Sciences,
Ulaanbaatar 210357, Mongolia

## Introduction

The Central Asian Orogenic Belt (CAOB; Fig. 1), also termed the Altaid Tectonic Collage (Sengör et al. 1993), is a complex tectonic mosaic of subduction-related complexes, island arcs, ophiolitic assemblages and slivers or terranes of Precambrian crystalline basement. The development and amalgamation of these orogenic domains are related to subduction-accretion processes within the Palaeo-Asian Ocean from early Neoproterozoic to late Palaeozoic time (Sengör et al. 1993; Buslov et al. 2001; Badarch et al. 2002; Khain et al. 2003; Kröner et al. 2007; Windley et al. 2007).

A striking feature of the CAOB is the predominantly juvenile character of the newly formed crust as revealed by Nd isotopic studies from Palaeozoic arc-related magmatic rocks (e.g., Jahn et al. 2000; Kovalenko et al. 2004; Helo et al. 2006). However, the concept of juvenile crust defined exclusively by Nd isotopic data may not always be correct as suggested by Hargrove et al. (2006) from a study of granitoids in the Arabian–Nubian Shield. These authors demonstrated that isotopically juvenile magmas assimilated significant amounts of old crustal material as revealed by large proportions of inherited zircon within these rocks. In a similar way, Precambrian ages documented by xenocrystic and detrital zircons from Palaeozoic felsic volcanic rocks and

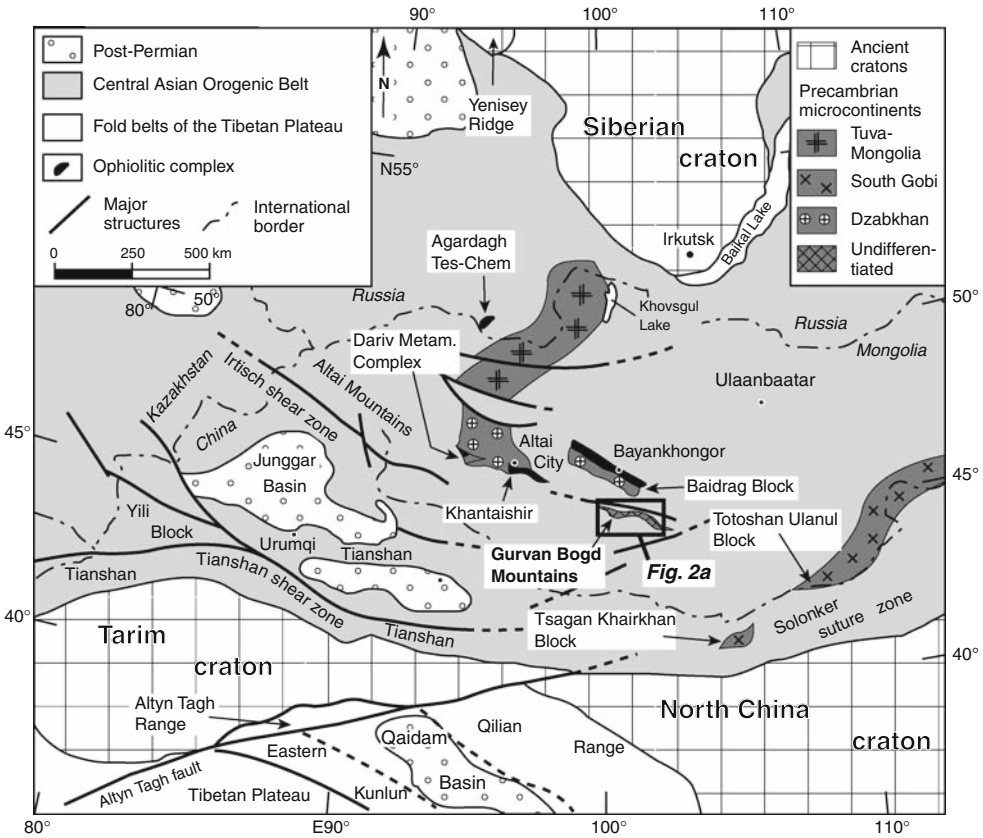


**Fig. 1** Sketch map showing the position of Mongolia within the Central Asian Orogenic Belt (modified after Jahn et al. 2000; Lu et al. 2008). The Central Asian Orogneic Belt (*light grey*) is predominantly composed of early Neoproterozoic to late Palaeozoic rock assemblages. The main identified Precambrian microcontinents, and their inferred extension, in Mongolia, northern China and southern Siberia are shown in *dark grey* (adapted from Kozakov et al. 2007). The ophiolitic complexes mentioned in this paper are shown in black. Location of Fig. 2a is also shown

arc-related clastic sediments in northern and central Mongolia (Kröner et al. 2007) suggest a substantial involvement of old material during the generation of these rocks.

Within most parts of the CAOB, and in particular Mongolia, terrains composed of high-grade metamorphic rocks were usually assumed to be Precambrian in age, though reliable radiometric ages are frequently missing (e.g., Mitrofanov et al. 1981; Badarch et al. 2002). These crystalline rocks were either interpreted as remnants of a single Precambrian microcontinent (Tuva-Mongolian; Sengör et al. 1993; Windley et al. 2007) or as individual microcontinents (e.g., Didenko et al. 1994 and references therein), namely Tuva-Mongolia, Dzabkhan and South Gobi. An alternative interpretation of the Tuva-Mongolia microcontinent (Kozakov et al. 1999; Salnikova et al. 2001) is based on U–Pb zircon ages which demonstrate that the earliest metamorphic event occurred at c. 536 Ma, followed by a regional phase of upper amphibolite-facies metamorphism between c. 497 and 489 Ma. These authors therefore suggested that discrete crustal domains, with distinct pre-metamorphic histories (Kozakov et al. 2005), were tectonically juxtaposed prior to c. 497 Ma and then underwent a phase of high-grade metamorphism as part of the evolution of the CAOB.

The existence of undoubted Precambrian crystalline rocks in central and southern Mongolia is documented by zircon dating for a variety of gneisses from the Baidrag (central Mongolia) and the Totoshan-Ulanul (southern Mongolia) blocks which are parts of the Dzabkhan and South Gobi microcontinents, respectively (Fig. 1). Within the Baidrag Block zircon dating yielded Archaean to Palaeoproterozoic emplacement ages of c. 2.80–1.82 Ga for orthogneiss protoliths (Mitrofanov et al. 1985; Kotov et al. 1995; Kröner et al. 2001; Kozakov et al. 2007), whereas early Neoproterozoic intrusion ages of c. 0.95 Ga characterize granitic protolith of gneisses from the Totoshan-Ulanul Block (Yarmolyuk et al. 2005).

We investigated the Baga Bogd massif in southern Mongolia, which is part of the Gurvan Bogd Mountain range (Fig. 1). The occurrence of high-grade metamorphic rocks, including granitic gneisses and migmatites, led this range to be considered as Precambrian in age (Badarch et al. 2002). This study focusses on SHRIMP zircon dating of a variety of granitoid gneisses in order to identify pre-Palaeozoic magmatic events and to possibly correlate the above rocks with other Precambrian crustal fragments in southern Mongolia.

## Geological framework

The Gurvan Bogd Mountain range is located at the eastern end of the Gobi-Altai in southwestern Mongolia and consists of three WNW–ENE striking massifs (Ih Bogd, Baga

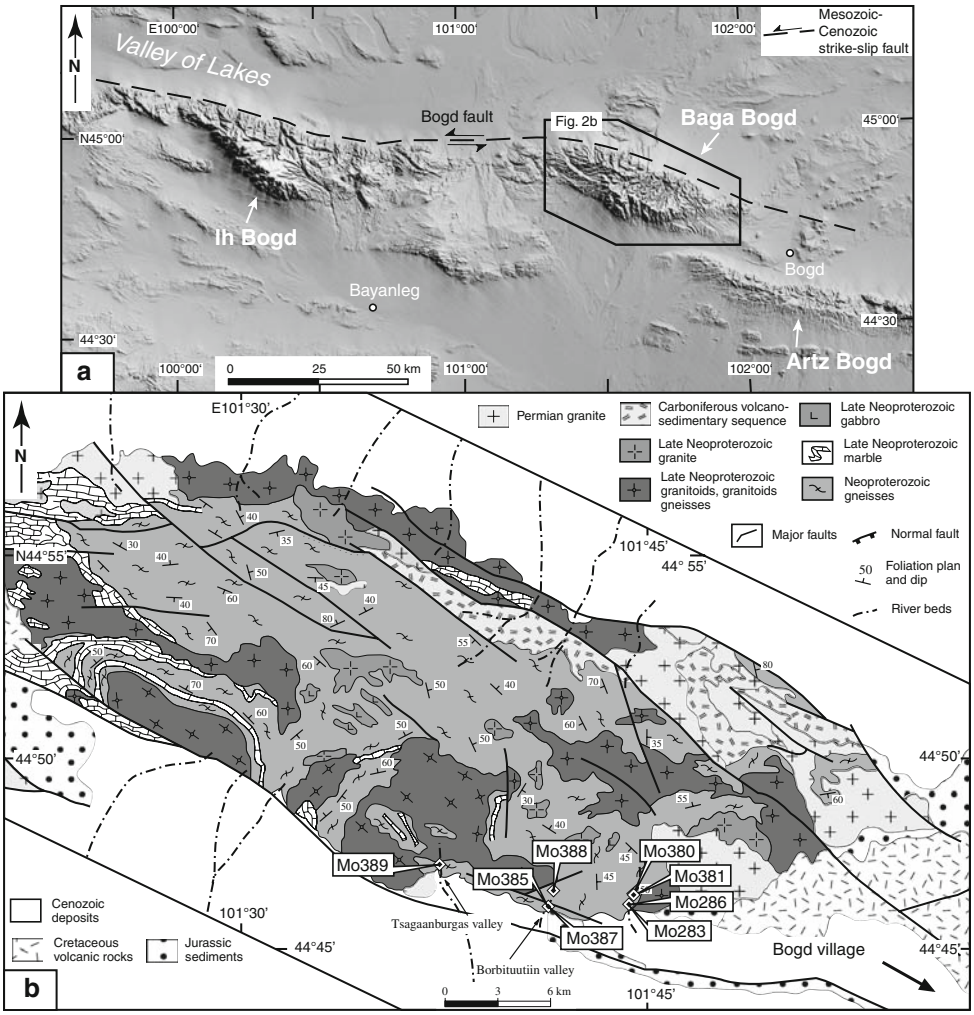


**Fig. 2** **a** Grey-scaled digital topographic map of the Gurvan Bogd Mountains showing the massif of interest for this study (Baga Bogd). **b** Geological sketch map of the Baga Bogd massif (modified after Geological Map L47-XXX, 1:200,000; Zabotkin 1988), with location of samples dated by SHRIMP

Bogd and Artz Bogd) with peaks up to 3,957 m (Fig. 2a). The present-day topography of this mountain system (and the Altai and Gobi-Altai regions in general) resulted primarily from Cenozoic transpressive deformation in response to far-field stresses associated with the Indo-Eurasian collision (Taponnier and Molnar 1979; Cunningham 2005). One of these massifs uplifted during this deformation is the Baga Bogd massif (Vassallo et al. 2007), an asymmetric elliptic massif bounded in the north by the left-lateral strike-slip Bogd fault (Bayasgalan et al. 1999). It consists predominantly of variably deformed and metamorphosed Precambrian rocks, intruded by late Neoproterozoic granitoids as inferred from the 1:200,000 geological map (Zabotkin 1988; Fig. 2b). Permian granitoids and Jurassic intracontinental sediments are locally found, whereas the northeastern part of the massif is characterized by the occurrence of a late Palaeozoic volcano-sedimentary sequence, which is mostly in tectonic contact with the metamorphic rocks.

Three N–S valleys have been investigated along the southern slope of the Baga Bogd massif, namely the Borbituutin and Tsagaanburgas valleys and a third, unnamed valley to the east (Fig. 2b). The rocks exposed along these valleys were deformed under upper greenschist- to amphibolite-facies metamorphism, locally leading to incipient migmatization. A strong penetrative foliation and tight folding affected all metamorphic rocks, leading to parallelism of most lithological contacts. Along the Tsagaanburgas valley, the predominant lithology is represented by strongly foliated dark augen-gneisses and layered migmatites of presumed igneous origin. These rocks are cut by undeformed dykes of mafic to intermediate composition, about one to several metres in width and consistently striking NE–SW and dipping from 45° to 75° NW or SE. The predominant rock types exposed along the Borbituutin and unnamed valleys are light grey augen-gneisses (Fig. 3a), layered migmatites (Fig. 3b), biotite-quartz-feldspar gneisses, and a higher proportion of clastic metasedimentary rocks, including metaquartzite and quartz-biotite schist, as compared to the Tsagaanburgas valley. Strongly foliated dioritic and granodioritic gneisses are also widespread in the unnamed valley. These rocks

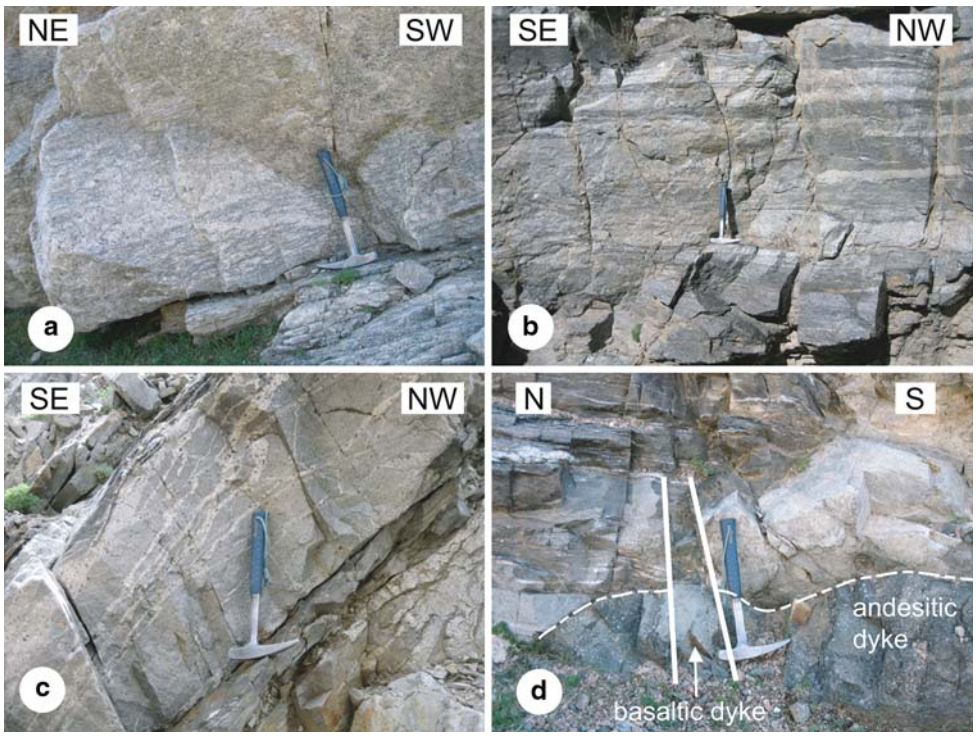


**Fig. 3** Field photographs of selected rock types from the Baga Bogd massif. **a** Strongly foliated light grey augen-gneiss (sample Mo385), Borbituutiin valley. **b** Banded migmatite, Borbituutiin valley. **c** Garnet-rich leucocratic veinlets cutting a fine-grained gneiss. **d** Cross-cutting relationship between basaltic/andesitic dykes and surrounding migmatitic country rock. Hammer for scale is 32 cm long

were, in turn, intruded by leucogranitic veins that locally display post-emplacement folding and boudinage; some veins contain a high proportion of garnet up to 1 cm in size (Fig. 3c). Undeformed dykes of mafic to intermediate composition (Fig. 3d), striking E–W and dipping S at 60–85°, also occur along these valleys.

## Sample description and geochronological results

Eight samples representing different varieties of granitoid gneisses were collected for SHRIMP zircon dating on the southern slope of the Baga Bogd massif (Fig. 2b). Separation of zircon grains followed standard procedures using heavy liquid and magnetic techniques. Representative zircons were hand-picked under a binocular microscope and mounted in epoxy resin together with chips of the reference zircons Temora 1 or CZ3. The resin disk was then polished to expose the interiors of the zircons. The internal structures of the grains were documented by cathodoluminescence (CL) images acquired with a JEOL JXA-8900 RL Superprobe in the Department of Geosciences, Mainz University (operating conditions were 15 kV accelerating voltage and 12 nA beam current on carbon-coated mounts). The U–Pb isotopic analyses on single zircons were carried out using the Sensitive High Resolution Ion Microprobe (SHRIMP II) at the Centre of Isotopic Research (CIR) in St. Petersburg (Russia) and in the Beijing SHRIMP Centre of the Chinese Academy of Geological Sciences. The instrumental characteristics are outlined by Larionov et al. (2004) and De Laeter and Kennedy (1998), respectively, and the analytical procedures are described in Claoué-Long et al. (1995), Nelson (1997) and Williams (1998). The uncertainty in the ratio $^{206}Pb^{*}/U$ during analysis of all CZ3 standard zircons during this study was 0.75% for the St. Petersburg instrument and 1.18% for the Temora 1 standard for the Beijing instrument. Sensitivity was about 56 cps/ppm/nA Pb for the standard CZ3 in St. Petersburg and about 23–24 cps/ppm/nA Pb for the Temora 1 standard on the Beijing instrument. The isotopic data and ages are reported in Table 1. Errors on individual analyses are given at the $1\sigma$ level, based on counting statistics, and include the uncertainty in the standard U/Pb age (Nelson 1997). Errors for pooled analyses are given at the 95% confidence interval. The ages and errors of intercepts of the best-fit line with concordia were calculated using the Isoplot program (Ludwig 2003). These errors were not multiplied by the square root of the MSWD since the absolute value of the intercept error is strongly model dependent.

Sample Mo283 is a dark and well-foliated, medium-grained dioritic orthogneiss collected in the unnamed valley (N44°45′58.9″, E101°44′35.6″). It represents the most dominant rock type in this valley and is composed of large biotite flakes, plagioclase, recrystallized quartz showing undulous extinction, and relicts of clinopyroxene. Accessory minerals include apatite, zircon and epidote. The rock shows a strong penetrative foliation, defined by biotite flakes, which conforms to the foliation developed in the surrounding fine-grained biotite gneiss and quartzo-feldspathic layered gneiss. Field relationships suggest the

**Table 1** SHRIMP isotopic results for single zircon grains of granitoid gneisses from the Baga Bogd massif

| Labels[a] | U (ppm) | Th (ppm) | $^{204}Pb/^{206}Pb$ | $^{208}Pb/^{206}Pb$ | $^{207}Pb/^{206}Pb$ | $^{206}Pb/^{238}U$ | $^{207}Pb/^{235}U$ | Age ± 1σ (Ma) | | |
|---|---|---|---|---|---|---|---|---|---|---|
| | | | | | | | | $^{206}Pb/^{238}U$ | $^{207}Pb/^{235}U$ | $^{207}Pb/^{206}Pb$ |
| Mo283[b] | | | | | | | | | | |
| 1.1 | 1374 | 35 | 0.00011 | 0.0086 ± 15 | 0.0577 ± 8 | 0.0804 ± 6 | 0.640 ± 10 | 499 ± 4 | 503 ± 6 | 520 ± 28 |
| 2.1 | 1622 | 295 | 0.00017 | 0.0740 ± 13 | 0.0614 ± 6 | 0.1072 ± 8 | 0.908 ± 12 | 656 ± 5 | 656 ± 6 | 654 ± 20 |
| 3.1 | 1132 | 1659 | 0.00003 | 0.4443 ± 30 | 0.0579 ± 8 | 0.0803 ± 6 | 0.641 ± 11 | 498 ± 4 | 503 ± 7 | 526 ± 30 |
| 4.1 | 1636 | 262 | 0.00003 | 0.0405 ± 11 | 0.0567 ± 6 | 0.0807 ± 6 | 0.631 ± 8 | 500 ± 4 | 497 ± 5 | 480 ± 22 |
| 5.1 | 668 | 410 | 0.00019 | 0.1957 ± 31 | 0.0571 ± 12 | 0.0803 ± 6 | 0.632 ± 14 | 498 ± 4 | 497 ± 9 | 494 ± 45 |
| 6.1 | 790 | 183 | 0.00007 | 0.0665 ± 15 | 0.0576 ± 7 | 0.0802 ± 6 | 0.636 ± 10 | 497 ± 4 | 500 ± 6 | 513 ± 28 |
| 7.1 | 689 | 498 | 0.00011 | 0.2192 ± 30 | 0.0578 ± 11 | 0.0804 ± 6 | 0.641 ± 13 | 498 ± 4 | 503 ± 8 | 524 ± 40 |
| 8.1 | 781 | 729 | 0.00017 | 0.2994 ± 39 | 0.0564 ± 14 | 0.0804 ± 6 | 0.624 ± 16 | 498 ± 4 | 493 ± 10 | 466 ± 52 |
| 9.1 | 625 | 235 | 0.00003 | 0.1211 ± 32 | 0.0575 ± 13 | 0.0803 ± 6 | 0.637 ± 16 | 498 ± 4 | 514 ± 6 | 580 ± 26 |
| Mo286[b] | | | | | | | | | | |
| 1.1 | 1100 | 2357 | 0.00001 | 0.6597 ± 17 | 0.0572 ± 4 | 0.0762 ± 9 | 0.601 ± 9 | 473 ± 5 | 478 ± 5 | 499 ± 14 |
| 2.1 | 1348 | 2993 | 0.00001 | 0.6856 ± 16 | 0.0571 ± 3 | 0.0776 ± 9 | 0.611 ± 8 | 482 ± 6 | 484 ± 5 | 497 ± 12 |
| 3.1 | 1672 | 2627 | 0.00020 | 0.4864 ± 15 | 0.0572 ± 4 | 0.0785 ± 9 | 0.619 ± 9 | 487 ± 6 | 489 ± 6 | 501 ± 16 |
| 4.1 | 1406 | 52 | 0.00003 | 0.0107 ± 7 | 0.0572 ± 4 | 0.0761 ± 9 | 0.600 ± 9 | 473 ± 5 | 477 ± 5 | 498 ± 14 |
| 5.1 | 1162 | 19 | <0.00001 | 0.0057 ± 2 | 0.0572 ± 3 | 0.0793 ± 10 | 0.625 ± 8 | 492 ± 6 | 493 ± 5 | 499 ± 11 |
| Mo380[c] | | | | | | | | | | |
| 1.1 | 390 | 214 | 0.00011 | 0.1908 ± 19 | 0.0578 ± 7 | 0.0803 ± 10 | 0.640 ± 12 | 498 ± 6 | 503 ± 7 | 524 ± 27 |
| 2.1 | 392 | 487 | 0.00017 | 0.3958 ± 25 | 0.0573 ± 8 | 0.0815 ± 11 | 0.643 ± 13 | 505 ± 6 | 504 ± 8 | 502 ± 31 |
| 3.1 | 1279 | 339 | 0.00003 | 0.0820 ± 4 | 0.0700 ± 2 | 0.1535 ± 20 | 1.481 ± 20 | 920 ± 11 | 923 ± 8 | 929 ± 6 |
| 4.1 | 566 | 148 | 0.00003 | 0.0900 ± 7 | 0.0688 ± 3 | 0.1481 ± 19 | 1.405 ± 20 | 890 ± 10 | 891 ± 9 | 893 ± 10 |
| 5.1 | 332 | 56 | 0.00019 | 0.1174 ± 18 | 0.0696 ± 8 | 0.1526 ± 20 | 1.464 ± 27 | 915 ± 11 | 916 ± 11 | 917 ± 23 |
| 6.1 | 320 | 36 | 0.00007 | 0.0385 ± 11 | 0.0662 ± 6 | 0.1347 ± 18 | 1.229 ± 20 | 815 ± 11 | 814 ± 8 | 813 ± 18 |
| Mo381[c] | | | | | | | | | | |
| 1.1 | 158 | 288 | 0.00020 | 0.5526 ± 29 | 0.0948 ± 9 | 0.2664 ± 35 | 3.484 ± 60 | 1523 ± 18 | 1524 ± 14 | 1525 ± 18 |
| 2.1 | 290 | 257 | 0.00007 | 0.2797 ± 15 | 0.0944 ± 5 | 0.2231 ± 29 | 2.903 ± 43 | 1298 ± 15 | 1383 ± 11 | 1516 ± 11 |
| 3.1 | 459 | 97 | 0.00019 | 0.0521 ± 13 | 0.0949 ± 6 | 0.2436 ± 32 | 3.188 ± 49 | 1405 ± 17 | 1454 ± 12 | 1527 ± 13 |
| 4.1 | 885 | 853 | 0.00062 | 0.3494 ± 17 | 0.0942 ± 7 | 0.1877 ± 24 | 2.438 ± 39 | 1109 ± 13 | 1254 ± 11 | 1512 ± 14 |
| Mo385[c] | | | | | | | | | | |
| 1.1 | 427 | 79 | <0.00001 | 0.0599 ± 8 | 0.0710 ± 6 | 0.1548 ± 18 | 1.517 ± 23 | 928 ± 10 | 937 ± 9 | 959 ± 16 |
| 2.1 | 608 | 160 | 0.00001 | 0.0710 ± 10 | 0.0707 ± 5 | 0.1510 ± 18 | 1.472 ± 22 | 907 ± 10 | 919 ± 9 | 948 ± 16 |
| 3.1 | 435 | 69 | <0.00001 | 0.0506 ± 7 | 0.0713 ± 5 | 0.1584 ± 19 | 1.557 ± 23 | 948 ± 11 | 953 ± 9 | 965 ± 15 |
| 4.1 | 387 | 145 | 0.00002 | 0.1344 ± 21 | 0.0707 ± 9 | 0.1403 ± 17 | 1.368 ± 25 | 846 ± 10 | 875 ± 11 | 949 ± 26 |
| 5.1 | 264 | 113 | <0.00001 | 0.1334 ± 16 | 0.0709 ± 7 | 0.1590 ± 19 | 1.554 ± 25 | 951 ± 11 | 952 ± 10 | 953 ± 19 |
| 6.1 | 384 | 83 | <0.00001 | 0.0678 ± 10 | 0.0708 ± 6 | 0.1395 ± 17 | 1.362 ± 21 | 842 ± 9 | 873 ± 9 | 952 ± 17 |
| Mo387[c] | | | | | | | | | | |
| 1.1 | 441 | 193 | 0.00075 | 0.0701 ± 27 | 0.0719 ± 12 | 0.1631 ± 21 | 1.617 ± 36 | 974 ± 12 | 977 ± 14 | 984 ± 34 |
| 2.1 | 421 | 152 | 0.00008 | 0.0711 ± 13 | 0.0718 ± 6 | 0.1197 ± 16 | 1.185 ± 19 | 729 ± 9 | 794 ± 9 | 982 ± 17 |
| 3.1 | 749 | 340 | 0.00004 | 0.0699 ± 7 | 0.0719 ± 3 | 0.1547 ± 20 | 1.533 ± 22 | 927 ± 11 | 944 ± 9 | 982 ± 10 |
| 4.1 | 659 | 241 | 0.00004 | 0.0707 ± 7 | 0.0719 ± 4 | 0.1484 ± 19 | 1.471 ± 21 | 892 ± 11 | 919 ± 9 | 984 ± 10 |
| 5.1 | 119 | 67 | 0.00010 | 0.0958 ± 16 | 0.1042 ± 8 | 0.3013 ± 40 | 4.330 ± 70 | 1698 ± 20 | 1699 ± 13 | 1701 ± 14 |
| Mo388[c] | | | | | | | | | | |
| 1.1 | 274 | 113 | 0.00033 | 0.0625 ± 35 | 0.0573 ± 15 | 0.0806 ± 11 | 0.637 ± 19 | 500 ± 6 | 501 ±12 | 504 ± 57 |
| 2.1 | 345 | 235 | 0.00022 | 0.0866 ± 25 | 0.0583 ± 11 | 0.0807 ± 11 | 0.648 ± 15 | 500 ± 6 | 507 ± 9 | 541 ± 40 |
| 3.1 | 254 | 136 | 0.00024 | 0.1031 ± 30 | 0.0577 ± 13 | 0.0814 ± 11 | 0.647 ± 17 | 504 ± 6 | 507 ±11 | 519 ± 48 |
| 4.1 | 333 | 220 | 0.00024 | 0.1141 ± 28 | 0.0568 ± 12 | 0.0807 ± 11 | 0.632 ± 16 | 500 ± 6 | 497 ±10 | 483 ± 45 |
| 5.1 | 792 | 368 | 0.00007 | 0.0812 ± 11 | 0.0577 ± 5 | 0.0813 ± 11 | 0.646 ± 10 | 504 ± 6 | 506 ± 6 | 518 ± 18 |

**Table 1** continued

| Labels[a] | U (ppm) | Th (ppm) | $^{204}Pb/^{206}Pb$ | $^{208}Pb/^{206}Pb$ | $^{207}Pb/^{206}Pb$ | $^{206}Pb/^{238}U$ | $^{207}Pb/^{235}U$ | Age ± 1σ (Ma) | | |
|---|---|---|---|---|---|---|---|---|---|---|
| | | | | | | | | $^{206}Pb/^{238}U$ | $^{207}Pb/^{235}U$ | $^{207}Pb/^{206}Pb$ |
| Mo389[c] | | | | | | | | | | |
| 1.1 | 419 | 92 | 0.00001 | 0.0631 ± 14 | 0.0711 ± 8 | 0.1601 ± 19 | 1.569 ± 28 | 957 ± 11 | 958 ± 11 | 960 ± 23 |
| 2.1 | 652 | 75 | <0.00001 | 0.0322 ± 7 | 0.0708 ± 6 | 0.1493 ± 18 | 1.458 ± 23 | 897 ± 10 | 913 ± 10 | 952 ± 19 |
| 3.1 | 676 | 91 | <0.00001 | 0.0387 ± 6 | 0.0709 ± 5 | 0.1468 ± 17 | 1.436 ± 20 | 883 ± 10 | 904 ± 8 | 956 ± 13 |
| 4.1 | 562 | 84 | <0.00001 | 0.0478 ± 7 | 0.0710 ± 5 | 0.1363 ± 16 | 1.334 ± 20 | 824 ± 9 | 861 ± 8 | 958 ± 15 |
| 5.1 | 1199 | 233 | <0.00001 | 0.0562 ± 5 | 0.0709 ± 3 | 0.1721 ± 20 | 1.681 ± 22 | 1024 ± 11 | 1002 ± 8 | 953 ± 10 |
| 6.1 | 446 | 64 | 0.00001 | 0.0450 ± 11 | 0.0709 ± 7 | 0.1402 ± 17 | 1.370 ± 22 | 846 ± 9 | 876 ± 9 | 954 ± 19 |
| 7.1 | 654 | 77 | <0.00001 | 0.0374 ± 6 | 0.0710 ± 5 | 0.1350 ± 16 | 1.321 ± 19 | 816 ± 9 | 855 ± 8 | 957 ± 14 |

[a] 1.1 is spot 1 on grain 1, 2.1 is spot 1 on grain 2, etc

[b] U–Th–Pb isotopic data obtained in St. Petersburg

[c] U–Th–Pb isotopic data obtained in Beijing

dioritic gneiss to be intrusive into the above gneisses, but the strong ductile deformation has largely obliterated the original contacts. This sample contains a population of zircons dominated by clear, euhedral and long prismatic grains with short and slightly rounded terminations. The colour varies from slight yellowish to pinkish, and the grain size ranges from 150 μm up to 300 μm in length. The grains display oscillatory zoning in CL images (Fig. 4a), characteristic of igneous growth. A few smaller grains <150 μm in length are also present and are characterized by a dark colour, short prismatic and subhedral habit with slightly rounded faces. Nine grains were analysed on the

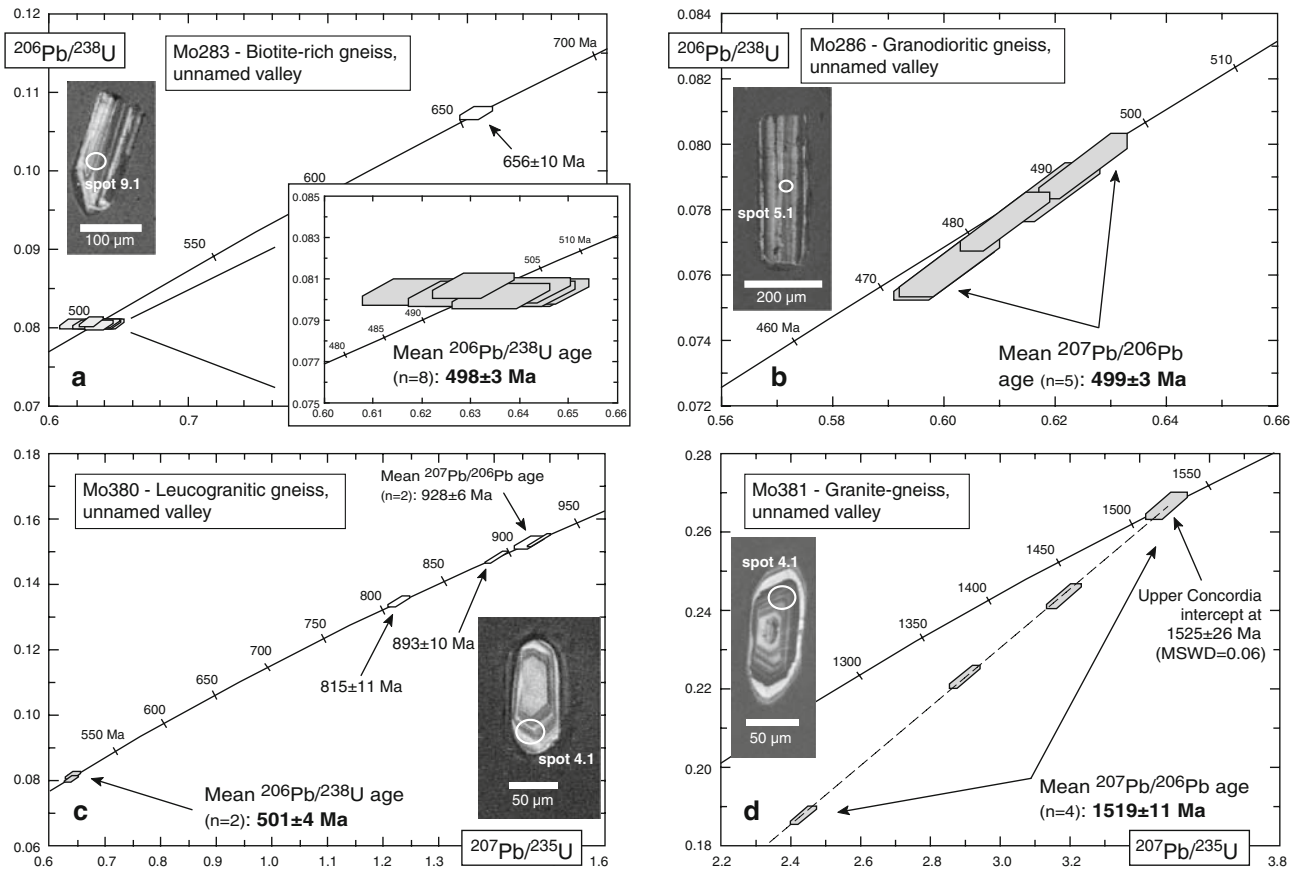


**Fig. 4** Concordia diagrams showing SHRIMP analyses of single zircons for samples from the unnamed valley. Data boxes for each analysis are defined by standard errors in $^{207}Pb/^{235}U$, $^{206}Pb/^{238}U$ and $^{207}Pb/^{206}Pb$. Errors on pooled ages are given at 95% confidence level. Insets show CL images of zircon grains, *white circles* indicate SHRIMP analytical spots; spot numbers refer to Table 1

St. Petersburg SHRIMP II (Table 1). Eight grains yielded a tight cluster of concordant results (Fig. 4a) with a weighted mean $^{206}Pb/^{238}U$ age of 498 ± 3 Ma which is interpreted to reflect the time of crystallization of the gneiss protolith. One grain yielded a significantly older, concordant result (Fig. 4a) with a $^{206}Pb/^{238}U$ age of 656 ± 10 Ma and is interpreted as a xenocryst, probably inherited from the basement rock into which the gneiss protolith was emplaced.

Sample Mo286 was collected some 15 m from sample Mo283 and is a strongly foliated, medium-grained biotite gneiss, originally a granodiorite, into which the above dioritic gneiss may originally have been intrusive. The texture is lepidoblastic, and the rock contains small biotite flakes mostly altered into chlorite, plagioclase with polysynthetic twinning, K-feldspar with a high degree of alteration and quartz showing undulous extinction. It contains accessory apatite, zircon, epidote and an oxide phase. The original relationship with the surrounding rocks is not clear since they now share the same foliation, and undoubted cross-cutting relationships are not preserved. The zircons from this sample are translucent, yellowish to slightly reddish in colour and predominantly long-prismatic or needle-like in shape and between 100 and 250 μm in length. Cathodoluminescence images reveal simple oscillatory zoning indicative of a magmatic origin and do not show inherited cores or metamorphic overgrowth (Fig. 4b). Five zircon grains were analysed on the St. Petersburg SHRIMP II (Table 1), and these produced concordant or near-concordant results (Fig. 4b) with a weighted mean $^{207}Pb/^{206}Pb$ age of 499 ± 3 Ma. We interpret this to reflect the time of emplacement of the granodioritic protolith. Both samples Mo283 and Mo286 obviously reflect the same magmatic event and may represent one phase of late Cambrian granitoid plutonism in the Baga Bogd massif.

Sample Mo380 is a leucocratic, fine-grained biotite granite-gneiss cut by garnet-rich leucogranitic veins and was collected higher up in the unnamed valley (N44°46′11.7″, E101°44′41.0″), some 400 m north of samples Mo283 and Mo286. It is composed of plagioclase, quartz, microcline, and small biotite flakes. The zircon grains are translucent, subhedral, long- to short-prismatic with a dominant brownish colour and vary in length between 100 and 250 μm. Cathodoluminescence images for the long-prismatic grains display simple igneous-related oscillatory zoning, whereas short-prismatic and more rounded grains tend to have partly recrystallized rims and convolute internal zoning (Corfu et al. 2003). Six grains were analysed on the Beijing SHRIMP II (Table 1) and produced concordant or near-concordant results which are spread along the concordia from 930 to 500 Ma (Fig. 4c). At the lowest end of the spread, two grains yielded concordant results, identical within error, with a mean $^{206}Pb/^{238}U$ age of 501 ± 4 Ma (Fig. 4c). The four remaining grains have ages between 930 and 815 Ma (Fig. 4c) with two grains at the end of the spread yielding similar results with a mean $^{207}Pb/^{206}Pb$ age of 928 ± 6 Ma. In view of the igneous origin of the zircons the age of 501 ± 4 Ma is interpreted as the time of emplacement of the gneiss precursor, whereas the remaining older grains suggest inheritance and involvement of Neoproterozoic basement material in the generation of the gneiss protolith. If this interpretation is correct, the gneiss protolith belongs to the same magmatic pulse as samples Mo283 and Mo286.

Sample Mo381 was collected in the same valley, about 600 m north of Mo380, and is a strongly foliated, fine-grained granite-gneiss composed of biotite and muscovite flakes, quartz, K-feldspar and garnet. K-feldspar is moderately to intensely sericitized, and garnet is extensively replaced by chlorite. The rock has a lepidoblastic texture defined by alternation of quartzo-feldspatic and micaceous bands. The sample contains a small population of subhedral, translucent and brownish zircons, and CL images reveal oscillatory zoning as well as partially recrystallized rims for most of the grains (Fig. 4d). Four zircons from this sample were analysed on the Beijing SHRIMP II (Table 1). One grain yielded a concordant analysis, and the three remaining grains produced discordant results (Fig. 4d). However, all analyses are aligned along a chord (MSWD = 0.06) yielding an upper intercept age of 1525 ± 26 Ma and a lower intercept at 60 ± 170 Ma reflecting recent lead-loss. All analyses have a weighted mean $^{207}Pb/^{206}Pb$ age of 1519 ± 11 Ma, identical within error to the upper intercept age, which we consider to best approximate the time of emplacement of the granitic protolith. Although sample Mo381 exhibits the same foliation as the other rocks described above, it is clearly much older and must be part of the basement into which the late Cambrian pluton was emplaced.

Sample Mo385 is a light grey augen-gneiss representing the main lithology in Borbituutiin valley and was collected at N44°46′05.3″, E101°41′29.0″. The gneiss is strongly foliated, coarse-grained, and is composed of quartz, microcline and millimetre-size biotite that is mostly altered into chlorite. K-feldspar is extensively sericitized, and the augen are up to 5 cm in size. The zircons are translucent, long- to short-prismatic, with variable aspects ratios and rounded terminations. The length ranges from 100 to 280 μm, and the colour varies from light to dark brown. Cathodoluminescence images reveal oscillatory zoning (Fig. 5a), characteristic of magmatic growth, and the presence of inherited cores in some grains. Six zircons were analysed on the Beijing SHRIMP II (Table 1) and display variable degrees of discordance (Fig. 5a). All

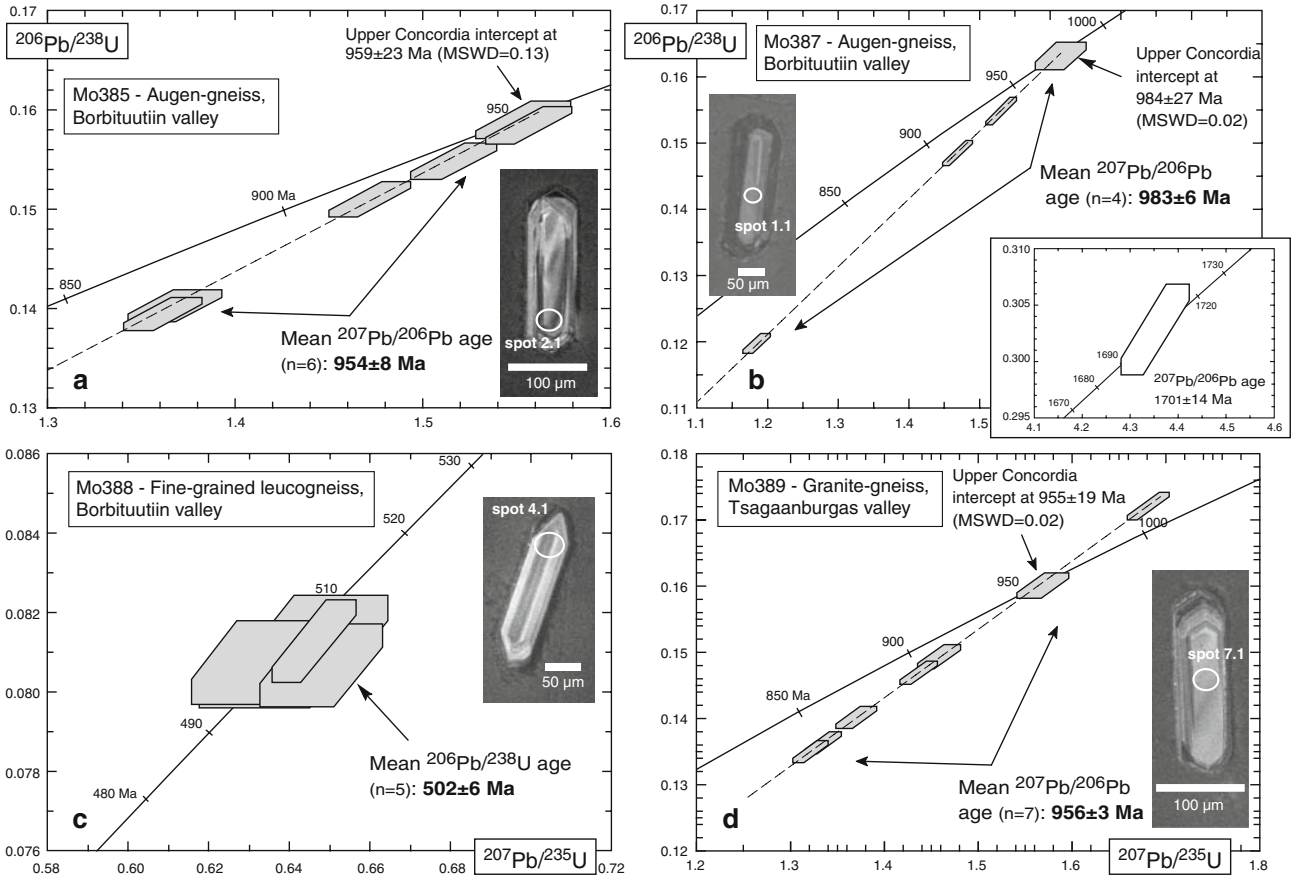


**Fig. 5** Concordia diagrams showing SHRIMP analyses of single zircons for samples from the Borbituutiin and Tsagaanburgas valleys. Data boxes for each analysis and errors on pooled ages as in Fig. 4. Insets show CL images of zircon grains, *white circles* indicate SHRIMP analytical spots; spot numbers refer to Table 1

analyses, with one virtually concordant, are well aligned along a chord (MSWD = 0.13) (Fig. 5a) and define a weighted mean $^{207}Pb/^{206}Pb$ age of 954 ± 8 Ma. The above chord defines an upper concordia intercept age of 959 ± 23 Ma and a lower intercept at 89 ± 330 Ma. The upper intercept age is identical to the mean $^{207}Pb/^{206}Pb$ age but less precise because of the large error in the lower intercept. This lower intercept is geologically meaningless and clearly reflects recent lead-loss. We therefore consider the mean $^{207}Pb/^{206}Pb$ age of 954 ± 8 Ma to most closely approximate the time of emplacement of the gneiss precursor. Again, this sample is part of a Precambrian basement.

Sample Mo387 is a medium-grained dark grey augen-gneiss collected farther north in Borbituutin valley at N44°46′12.0″, E101°41′33.5″. It is composed of strongly seriticized K-feldspar porphyroblasts, quartz, and biotite flakes with chloritized rims. It has a grano-lepidoblastic texture with a gneissic fabric underlined by biotite and quartz ribbons. The zircons are long-prismatic with a high aspect ratio, or short-prismatic and are translucent, mostly subhedral with rounded edges and light grey to brown colour. Cathodoluminescence images reveal well developed oscillatory zoning due to igneous growth (Fig. 5b) and core-rim relationships in some grains. Five zircon grains from this sample were analysed on the Beijing instrument (Table 1). Four concordant and discordant analyses (Fig. 5b) are aligned along a discordia line (MSWD = 0.02) which defines a lower intercept at 8 ± 190 Ma and an upper intercept age of 984 ± 27 Ma, identical within error to the weighted mean $^{207}Pb/^{206}Pb$ age of 983 ± 6 Ma of the four analyses. Thus, the age of 983 ± 6 Ma is considered to reflect the time of emplacement of the granitic protolith. The fifth grain yielded a much older $^{207}Pb/^{206}Pb$ age of 1701 ± 14 Ma ($1\sigma$) (Fig. 5b), which, as in previous samples, is interpreted as a xenocryst inherited from a late Palaeoproterozoic crustal source.

Sample Mo388 is a strongly deformed very fine-grained, laminated leucocratic gneiss, interlayered with the surrounding augen-gneiss and collected still farther north in Borbituutin valley at N44°47′03.5″, E101°41′14.1″. The

mineral assemblage consists of K-feldspar, quartz and minor biotite flakes. The zircons are of two types. Type 1 is represented by clear, transparent, long- to short-prismatic and euhedral grains, 100–150 μm in length and displaying typical magmatic growth features under cathodoluminescence (Fig. 5c). Type 2 grains are mostly short-prismatic, subhedral with rounded terminations and dark brown colour. They range in length between 100 and 250 μm and display complex internal growth structures as revealed by CL images. Five grains of type 1 grains were analysed on the Beijing SHRIMP II (Table 1) and yielded concordant results (Fig. 5c) with a weighted mean $^{206}Pb/^{238}U$ age of 502 ± 6 Ma which we interpret as the time of emplacement of the gneiss protolith.

Lastly, sample Mo389 is a coarse-grained, light grey granite-gneiss collected in Tsagaanburgas valley at N44°47′29.8″, E101°37′16.9″. This gneiss is composed of large K-feldspar, quartz, minor plagioclase, millimetre-size biotite and large idiomorphic garnet crystals altered into an assemblage of chlorite + quartz. K-feldspar is moderately sericitized and biotite is mostly transformed into chlorite. Quartz is mostly recrystallized. The zircons are mainly short-prismatic with rare long-prismatic and transparent grains. Most grains are euhedral to subhedral with slightly rounded terminations, vary in length from 80 to 250 μm, and are light yellowish to dark brownish in colour. Cathodoluminescence images reveal well-developed oscillatory zoning (Fig. 5d), characteristic of igneous crystallization, and do not show cores or overgrowth. Seven zircons were analysed on the Beijing instrument and yielded well-aligned results one of which is concordant, one reversely discordant and five exhibit variable degrees of discordance (Table 1; Fig. 5d). All analyses define a weighted mean $^{207}Pb/^{206}Pb$ age of 956 ± 3 Ma, whereas linear regression (MSWD = 0.02) resulted in an upper concordia intercept age of 955 ± 19 Ma and a lower intercept at −13 ± 240 Ma which clearly reflects recent Pb-loss. As in the case of sample Mo385, both ages are identical, and we consider the more precise mean $^{207}Pb/^{206}Pb$ age as most closely reflecting the time of protolith emplacement.

## Whole-rock major and trace elements chemistry

Major and trace element data for the dated samples were obtained by X-ray fluorescence spectrometry, using a Philips MagiXPro spectrometer in the Department of Geosciences, Mainz University. Loss on ignition (LOI) was determined by weight loss after heating at 1050°C for 4 h. The results are listed in Table 2.

Zircon geochronology revealed three groups of ages, one at around 500 Ma (samples Mo283, Mo286, Mo380 and Mo388), another with early Neoproterozoic ages ranging from 983 to 954 Ma (samples Mo385, Mo387 and Mo389) and one with a much older age of 1.52 Ga (sample Mo381). The distinction between the three groups was already suspected from field relationships although intrusive features displayed by the youngest group were partly obliterated during post-intrusion deformation. In the following, these samples will be treated as two separate groups: Precambrian (Meso- and early Neoproterozoic) gneisses on one side and the late Cambrian gneisses on the other side. The chemical indices of alteration (CIA; Table 2) of 46–55 for all granitoid gneisses are comparable to those of unaltered granitic and mafic rocks (CIA for average fresh granite: 45–55; Nesbitt and Young 1982) except for the granite gneiss Mo381 which has a CIA index of 69 and the highest LOI value of 1.75 (Table 2). Nevertheless, the relatively high degree of alteration of K-feldspar and some biotite observed in thin section indicates that some elements and the alkaline elements in particular, may not reflect primary compositions.

### Major element chemistry

The early Neoproterozoic gneisses are granitic and calc-alkaline in composition (Fig. 6; Table 2) and show limited variation in chemical composition with restricted $SiO_2$ contents of c. 71–79 wt% (Table 2). They are characterized by homogeneous and low $TiO_2$, $Fe_2O_3t$, MgO and CaO contents and relatively high $K_2O$ contents of 5.6–6.4 wt% (Table 2), whereas significant scatter is observed for $Al_2O_3$, $Na_2O$ and $P_2O_5$ (Table 2). These samples are all slightly peraluminous with A/CNK (Aluminium Saturation Index; molecular $Al_2O_3/(CaO + Na_2O + K_2O)$ and A/NK values of 1.1 and 1.2–1.3, respectively (Fig. 7a; Table 2). Compared to these samples, the Mesoproterozoic gneiss has lower $SiO_2$, CaO, $Na_2O$, $K_2O$, $P_2O_5$ contents and higher $Al_2O_3$, $Fe_2O_{3t}$, MgO and $TiO_2$ contents (Table 2). This sample is clearly peraluminous (Fig. 7a; Table 2) with A/CNK and A/NK values of 2.2 and 2.6, respectively, in agreement with its mineralogy. All samples with Precambrian ages are moreover characterized by low $Na_2O/K_2O$ ratios (0.3–0.5) and an enrichment in iron as suggested by $FeO_t/(FeO_t + MgO)$ ratios that are systematically higher than 0.8 at a given $SiO_2$ content (Fig. 7b).

The late Cambrian gneisses cover a wide compositional range with $SiO_2$ contents of c. 55–68 wt% (Table 2) and show dioritic to granodioritic compositions with calk-alkaline affinities (Fig. 6). They display crude correlations of decreasing $TiO_2$, $Fe_2O_{3t}$, MgO and CaO with increasing $SiO_2$ (Table 2). Most gneisses are slightly peraluminous with A/CNK and A/NK values of 1.1–1.2 and 1.5–1.7, respectively (Fig. 7a; Table 2), whereas sample Mo283 with $SiO_2 < 56$ wt% is classified as metaluminous with

**Table 2** Major and trace element analyses of granitoid gneisses from the Baga Bogd massif

| Sample | Mo283 | Mo286 | Mo380 | Mo381 | Mo385 | Mo387 | Mo389 |
|---|---|---|---|---|---|---|---|
| Lithology[a] | Meta-D | Meta-GD | G-gneiss | G-gneiss | G-gneiss | G-gneiss | G-gneiss |
| Age (Ma) | 498 ± 3 | 499 ± 3 | 501 ± 4 | 1519 ± 11 | 954 ± 8 | 983 ± 6 | 956 ± 3 |
| $SiO_2$ | 55.30 | 64.08 | 68.41 | 64.11 | 78.73 | 71.36 | 71.35 |
| $TiO_2$ | 1.65 | 0.99 | 0.48 | 0.83 | 0.15 | 0.27 | 0.11 |
| $Al_2O_3$ | 15.99 | 16.76 | 14.78 | 18.55 | 10.74 | 14.1 | 14.32 |
| $Fe_2O_3t$ | 7.99 | 4.67 | 2.80 | 6.23 | 1.42 | 2.08 | 1.53 |
| MnO | 0.12 | 0.07 | 0.03 | 0.12 | 0.04 | 0.03 | 0.02 |
| MgO | 4.06 | 1.29 | 0.70 | 1.14 | 0.09 | 0.28 | 0.16 |
| CaO | 6.24 | 2.74 | 1.69 | 0.66 | 0.56 | 1.00 | 0.96 |
| $Na_2O$ | 2.26 | 3.79 | 2.90 | 1.57 | 1.79 | 2.71 | 2.91 |
| $K_2O$ | 3.05 | 4.23 | 4.90 | 4.13 | 5.61 | 6.27 | 6.36 |
| $P_2O_5$ | 0.94 | 0.37 | 0.16 | 0.05 | 0.18 | 0.07 | 0.07 |
| LOI | 1.40 | 0.77 | 0.83 | 1.75 | 0.52 | 0.38 | 0.71 |
| Total | 99.02 | 99.76 | 97.68 | 99.14 | 99.83 | 98.55 | 98.52 |
| CIA[b] | 46.6 | 51.5 | 52.9 | 69.2 | 51.7 | 51.9 | 51.6 |
| A/CNK[c] | 0.9 | 1.1 | 1.1 | 2.2 | 1.1 | 1.1 | 1.1 |
| A/NK[d] | 2.3 | 1.6 | 1.5 | 2.6 | 1.2 | 1.3 | 1.2 |
| Rb | 203 | 276 | 229 | 222 | 190 | 358 | 275 |
| Sr | 864 | 606 | 259 | 101 | 96 | 95 | 87 |
| Ba | 1056 | 1162 | 943 | 631 | 367 | 557 | 301 |
| Zr | 293 | 364 | 275 | 200 | 110 | 151 | 85 |
| Nb | 31 | 28 | 17 | 18 | 5 | 9 | 4 |
| Th | 14 | 39 | 47 | 17 | 9 | 30 | 24 |
| Pb | 22 | 43 | 53 | 34 | 38 | 50 | 54 |
| Cr | 77 | 3 | 7 | 61 | bd | 4 | 3 |
| Ni | 29 | 5 | 6 | 25 | 4 | bd | 4 |
| Y | 26 | 20 | 14 | 35 | 19 | 37 | 24 |
| V | 118 | 46 | 27 | 97 | bd | 16 | 6 |
| Sc | 15 | 7 | 3 | 13 | 3 | 3 | 3 |
| Co | 26 | 6 | 2 | 19 | bd | 3 | 2 |
| Cu | 21 | 6 | bd | 23 | 6 | bd | 6 |
| Zn | 124 | 96 | 55 | 85 | 16 | 37 | 24 |
| Ga | 22 | 22 | 21 | 24 | 16 | 19 | 22 |
| La | 82 | 74 | 53 | 29 | 18 | 36 | 19 |
| Ce | 163 | 154 | 91 | 61 | 27 | 68 | 35 |
| Pr | 21 | 17 | 11 | 8 | 2 | 10 | 8 |
| Nd | 71 | 58 | 38 | 31 | 15 | 30 | 18 |
| Sm | 4 | 8 | 8 | 10 | 3 | 8 | 4 |

Major and trace elements were measured by XRF and are in wt% and ppm, respectively

$Fe_2O_3t$ total iron as $Fe_2O_3$; *LOI* loss on ignition; *bd* below detection limit

[a] D, diorite; GD, granodiorite; G, granite

[b] CIA: molecular ratio $100*[Al_2O_3/(Al_2O_3+CaO + Na_2O + K_2O)]$

[c] A/CNK: molecular ratio $Al_2O_3/(CaO + K_2O + Na_2O)$

[d] A/NK: molecular ratio $Al_2O_3/(K_2O + Na_2O)$

A/CNK $< 1$ and A/NK $> 1$ (Fig. 7a; Table 2). Moreover, these samples have higher $Na_2O/K_2O$ ratios (0.6–1.2) and $FeO_t/(FeO_t + MgO)$ ratios systematically lower than 0.8 (Fig. 7b) and are referred to as magnesian Cordilleran-type granitoids according to the classification of Frost et al. (2001).

## Trace element chemistry

The Neoproterozoic granites gneisses have relatively low concentrations of Nb (4–9 ppm), Zr (85–151 ppm), Sr (87–96 ppm) and Ba (301–557 ppm). They show slight enrichments in large ion lithophile elements (LILE; Ba, Th, U) compared to high field strength elements (HFSE; Nb, Zr, Ti) and display Nb, Sr and Ti troughs on a bulk continental crust-normalized trace element patterns (Fig. 8a). The Mesoproterozoic gneiss Mo381 displays a slightly different picture with higher concentrations of Ba, Nb, Zr, Ni and Cr (Table 2). Trace elements normalized to bulk continental crust show an overall good agreement with typical crustal values except for lower concentrations in Sr and P (Fig. 8a). Using the Nb–Y trace-element

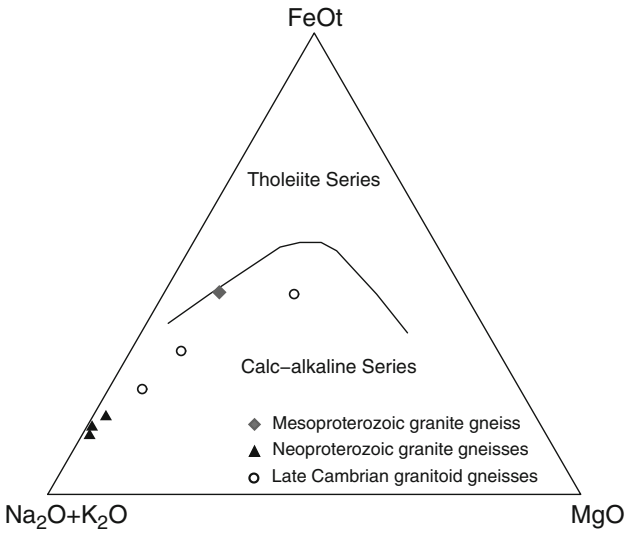


**Fig. 6** AFM diagram for gneisses from the Baga Bogd massif showing. FeOt, total iron as FeO; dividing line between tholeiitic and calc-alkaline series is from Irvine and Baragar (1971)

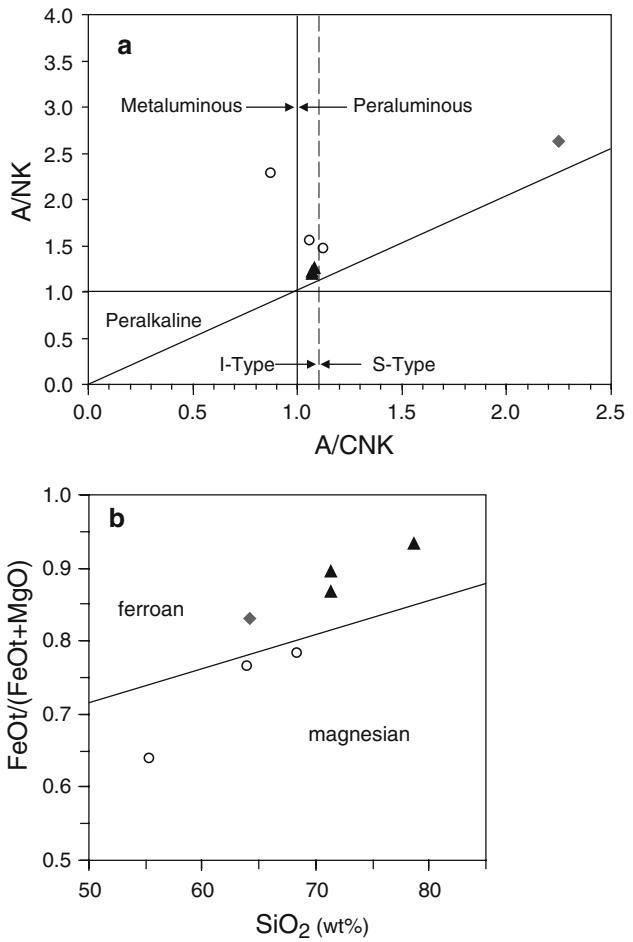


**Fig. 7** **a** A/NK vs A/CNK diagram, modified after Shand (1951) and **b** FeOt/(FeOt + MgO) versus $SiO_2$ diagram after Frost et al. (2001). FeOt, total iron as FeO. For legend see Fig. 6

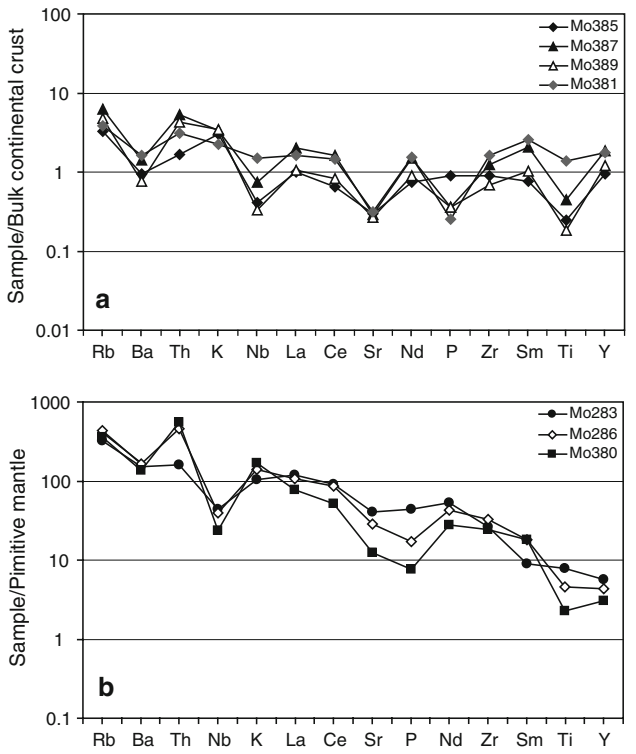


**Fig. 8** Multi-element diagrams for **a** Meso- and early Neoproterozoic gneisses and **b** late Cambrian gneisses from the Baga Bogd massif. All elements were analysed by XRF; primitive mantle and bulk continental crust normalizing values are from Sun and McDonough (1989) and Rudnick and Fountain (1995), respectively

discrimination diagram of Pearce et al. (1984), all Precambrian samples plot in the field of syn-collisional (syn-COLG)/volcanic arc-related granitoids (VAG, Fig. 9).

Compared to the Precambrian samples, the late Cambrian rocks are more enriched in Nb, Zr, Sr and Ba (Table 2).These samples are characterized by enrichment in LILE compared to HFSE when plotted in a primitive mantle-normalized spidergram (Fig. 8b). They display well pronounced negative Nb anomalies and slightly negative Ti anomalies. These gneisses display crude trends of decreasing contents of Nb, Sr, Ba and increasing Zr with increasing content of $SiO_2$ (Table 2). In the Nb–Y discrimination diagram (Fig. 9) (Pearce et al. 1984) these samples overlap the fields of syn-COLG/VAG and within-plate granitoids (WPG, Fig. 9), which suggests formation in an active continental margin environment or in a mature island arc.

## Discussion

Our SHRIMP zircon ages for granitoid protoliths of various orthogneisses from the Baga Bogd massif in southern Mongolia confirm the Neoproterozoic and Cambrian age

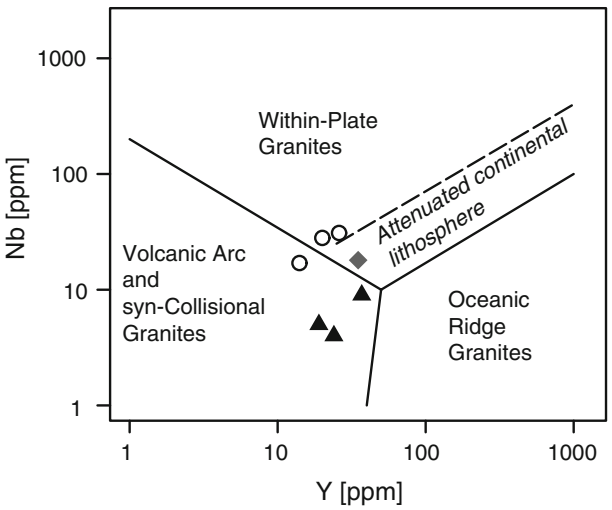


**Fig. 9** Nb versus Y discrimination diagram for granites after Pearce et al. (1984). For legend see Fig. 6

assessments inferred on the 1:200,000 geological map (Fig. 2b). We suspect that the Neoproterozoic gneisses experienced some structural and possibly metamorphic history prior to their incorporation into the early Palaeozoic arc terrane of southern Mongolia. However, strong ductile deformation during the Palaeozoic accretion event led to parallelism of structures in all metamorphosed rocks so that no distinction could be made in the field between Palaeozoic and older structures. No angular relationships between the Precambrian and early Palaeozoic orthogneisses were observed. This is unlike some of the low-strain domains of the large Baidrag Block farther NE where Precambrian structures and a polymetamorphic Precambrian history are well preserved (Kozakov et al. 2007).

## Precambrian thermal events and possible link to identified crustal basement

The oldest dated event in the geological evolution of the study area was the intrusion of the granitic gneiss precursor of sample Mo381 at 1519 ± 11 Ma. An even older age of c. 1700 Ma is documented by a xenocrystic zircon grain from grey augen-gneiss sample Mo387. These ages document the presence of late Palaeoproterozoic to early Mesoproterozoic crust in the Baga Bogd massif.

The existence of Precambrian crust of Archaean to Palaeoproterozoic age is well documented for the Baidrag Block (Dzabkhan microcontinent; Kozakov et al. 1997) which is located to the northwest of the study area (Fig. 1). The Baidrag basement shows a complex and polyphase tectono-metamorphic evolution from late Archaean to late Palaeoproterozoic time (e.g., Kozakov et al. 1997, 2007 and references therein). The oldest rocks correspond to tonalitic and two pyroxene gneisses with protolith emplacement ages documented by conventional multigrain and SHRIMP single zircon ages of c. 2.80–2.65 Ma (Mitrofanov et al. 1985; Kozakov et al. 2007). The last major thermal event experienced by these rocks reflects the peak of granulite-facies metamorphism with a minimum age of 1839 ± 1 Ma (Pb–Pb zircon evaporation age, Kröner et al. 2001), for metamorphic zircons from a metapelitic rocks. A post-tectonic granite with a U–Pb zircon age of 1825 ± 5 Ma (conventional method; Kotov et al. 1995) marks the final consolidation of this Precambrian crystalline block.

Other discrete Precambrian crustal domains are recognized in western Mongolia in the Dariv Metamorphic Complex and the Khantaishir Complex (Fig. 1), also assumed to be part of the Dzabkhan microcontinent (Badarch et al. 2002; Kozakov et al. 2002), but display slightly different age patterns in comparison to the Baidrag Block. Within the Dariv Metamorphic Complex there are unpublished zircon ages between 840 and 600 Ma with rare xenocrysts up to Archaean in age (Kozakov I.K., pers. comm., 2007). The minimum age of emplacement for the protolith of a dioritic gneiss is 1426 ± 1 Ma (Pb–Pb zircon evaporation age; Kröner et al. 2001). The Khantaishir Complex around Altai City contains a porphyritic granite-gneiss with a crystallization age of 1127 ± 1 Ma and a 1715 Ma old xenocrystic zircon (Pb–Pb zircon evaporation ages; Kröner et al. 2001). Near Altai City, a migmatite yielded a SHRIMP zircon age of 840 ± 9 Ma and also contains inherited zircons ranging from 2,445 to 1,440 Ma in age (Zhao et al. 2006).

Compared to the crustal fragments discussed above, a distinctive feature of the Baga Bogd massif are the early Neoproterozoic granitic intrusions documented by three samples (Mo387, Mo389, and Mo385) and yielding emplacement ages of 983 ± 6, 956 ± 3 and 954 ± 8 Ma, respectively. Granitic protholiths with early Neoproterozoic ages have so far only been identified in one locality in southern Mongolia. A granite-gneiss exposed in the Totoshan-Ulanul Block of south-eastern Mongolia (Fig. 1) provided a protolith intrusion age of 952 ± 8 Ma (conventional U–Pb single and multigrain zircon age; Yarmolyuk et al. 2005). A similar event was documented to the W of the Totoshan-Ulanul Block within the Tsagan-Khairkhan Block of northern China (Fig. 1) where emplacement of a granite-gneiss protolith was dated at 916 ± 16 Ma (U–Pb zircon age; Wang et al. 2001). These two blocks are usually considered as part of the South Gobi microcontinent.

The origin of these microcontinental crustal fragments is uncertain in most cases. They are interpreted either as fragments derived from the East Gondwana margin (Mossakovsky et al. 1993; Didenko et al. 1994; Filippova et al. 2001; Dobretsov et al. 2003; Dobretsov and Buslov

2007; Kheraskova et al. 2003) or from the Siberian craton (Berzin et al. 1994; Kuzmichev et al. 2001; Yarmolyuk et al. 2006) or from both (Buslov et al. 2001). However, late Mesoproterozoic to early Neoproterozoic magmatic events have not been documented so far from the Siberian craton margin (Pisarevsky and Natapov 2003; Gladkochub et al. 2006; Smelov and Timofeev 2007), and the distribution of sedimentary successions mainly record a passive margin environment (Pisarevsky et al. 2008). For example, the Teya granite pluton, part of the Yenisey Ridge and located at the south-western margin of the Siberian Craton (Fig. 1), has long been considered to reflect a Grenvillian-age collisional event. However, Vernikovsky et al. (2007) have now shown that the oldest phase of magmatism in this area occurred between 875 and 864 Ma, making a possible link with a Grenvillian-age event unlikely. On the other hand, discrete early Neoproterozoic magmatism is documented in northwestern China. Southeast of the Tarim Basin, the Qilian and Qaidam blocks (Fig. 1) host granitoids, which are intrusive into shallow marine strata and ultramafic rocks and yielded emplacement ages of c. 930–920 Ma (conventional U–Pb zircon ages; Gehrels et al. 2003), whereas a zircon age of c. 969 Ma was reported for a granitoid gneiss in the Altyn Tagh range (Fig. 1)(ion microprobe analysis; Cowgill et al. 2003). Lu et al. (2008) listed numerous zircon ages between 1,050 and 920 Ma for granitoids from the northern and eastern margin of the Tarim craton. These authors interpret these early Neoproterozoic magmatic events as the result of what they term "Tarimian Orogeny", leading to the final cratonization of the Tarim Craton.

The aforementioned magmatic ages compare well with our new zircon ages and suggest that the Baga Bogd massif is unlikely to be related to the Baidrag basement block but shares greater similarities with crustal fragments in southern Mongolia and northwestern China. It is therefore unlikely that the Baga Bogd block was derived from the Siberian craton. It may either be considered as a fragment of the South Gobi microcontinent, rifted off the northeastern Gondwana margin (Buslov et al. 2001) or as a fragment of the Tarim Craton. However, considering the poor correlation and the paucity of reliable ages, further data are required to draw definitive conclusions.

## Late Cambrian plutonism and geodynamic implications

Finally, our results document a phase of late Cambrian magmatism with the emplacement of granitic, granodioritic and dioritic intrusions at 502 ± 6, 501 ± 4, 499 ± 3 and 498 ± 3 Ma. Moreover, two of the late Cambrian gneisses contain xenocrystic zircons with ages of c. 928, 893, 815 and 656 Ma. These inherited grains provide further evidence for Neoproterozoic crustal material and suggest several Neoproterozoic zircon-forming events within the study area as also supported by early Neoproterozoic zircon ages recorded in samples Mo385, Mo387 and Mo389.

Evidence for an oceanic domain to the north of the Baidrag Block is indicated by the large (300 km long) Bayankhongor ophiolite mélange recording ocean-crust formation at c. 665 Ma ago (SHRIMP zircon age; Kovach et al. 2005). A minimum age for the accretion of this oceanic remnant with the Baidrag block (Buchan et al. 2001) is bracket by syn-collisional granitoids intruding the ophiolite and its boundary fault between c. 547 and 539 Ma (U–Pb and Pb–Pb zircon evaporation ages; Buchan et al. 2002; Kozakov et al. 2006). Within this interval, the southwestern margin of the Siberian craton faced the open Palaeo-Asian Ocean as indicated by a broad belt of c. 570 Ma old ophiolitic remnants. Slivers of oceanic crust are well exposed in the Khantaishir ophiolite south of Altai City (U–Pb zircon age of 568 ± 4 Ma for plagiogranite; Khain et al. 2003), in the Dariv range farther W (Bayannor ophiolite, U–Pb zircon age of 571 ± 4 Ma for plagiogranite; Khain et al. 2003) and more to the north in the Tuva area of southern Siberia with the Agadagh Tes-Chem Massif (Pb–Pb zircon evaporation age of 570 ± 1 Ma; Pfänder and Kröner 2004). The accretion of these portions of oceanic lithosphere onto Precambrian crystalline massifs likely occurred in late Cambrian time and was accompanied by widespread magmatism and regional metamorphism. A minimum time for the accretion of the Bayannor ophiolite within the Dariv Metamorphic Complex is given by the intrusion of an undeformed quartz diorite at 515 ± 8 Ma (SHRIMP zircon age; Dijkstra et al. 2006). A phase of high-grade metamorphism in this complex is moreover recorded at 499 ± 3 Ma by a U–Pb zircon age for a hypersthene-garnet granulite (Kozakov et al. 2002) and may reflect accretion of the ophiolitic sequence onto the crystalline basement. The post-tectonic intrusion of a "stitching granite" at 497 ± 1 Ma (Pb–Pb zircon evaporation age; Kröner et al. 2001) indicates that this phase of accretion was accomplished in the latest Cambrian.

Within this framework, and according to the chemistry of the dated samples, we consider that the late Cambrian phase of magmatism recorded in the Baga Bogd massif occurred in an active continental margin environment and was related to the progressive closure of the Palaeo-Asian Ocean. Moreover, these data suggest that the Baga Bogd Precambrian crustal fragment was either docked against the southward (present-day coordinates) growing margin of the CAOB or was a large enough crustal entity to develop a magmatic arc along its margin.

The field relationships, combined with our new zircon ages, indicate that the different generations of granitoid

gneisses underwent a common metamorphic and deformational event. This produced the regional penetrating fabric, leading to tectonic interlayering of Precambrian and late Cambrian gneisses, and most probably culminated in migmatization of the most fertile lithologies. This event occurred after the Cambrian, but our data are insufficient to constrain the time of post-Cambrian metamorphism. We speculate that this event may signify accretion of the Baga Bogd or South Gobi basement terrane onto the southward (present-day coordinates) growing margin of the CAOB or accretion of a Japan-style basement-core magmatic arc in the course of continuous closure of oceanic basins in the Palaeo-Asian Ocean.

## Conclusions

Our new SHRIMP zircon ages for granitoid gneisses in the Baga Bogd massif of southern Mongolia indicate the presence of Precambrian crystalline rocks and a late Cambrian phase of granitoid magmatism. The protolith emplacement of a granite-gneiss (Mo381) is dated at 1519 ± 11 Ma and represents, up to now, the oldest rocks in this massif. A phase of magmatism is then documented by granite-gneisses whose precursors were emplaced at 983 ± 6, 956 ± 3 and 954 ± 8 Ma. This is the second record in southern Mongolia of early Neoproterozoic granitoid magmatism. Finally, a late Cambrian subduction-related phase of magmatism is identified by several granitoid gneisses with homogeneous protolith intrusion ages at c. 500 Ma. Our results document the presence of an additional fragment of Precambrian crystalline basement in southern Mongolia and reinforce the idea that slivers of Precambrian crystalline domains are widespread in central and southern Mongolia as suggested by recent geological and isotopic studies (Yarmolyuk et al. 2005; Kozakov et al. 2007).

**Acknowledgments** This paper is part of a collaborative study with the Institute of Geology and Mineral Resources, Mongolian Academy of Sciences, and funded by the Volkswagen Foundation under grant I/76399 to A.K. A.D. and laboratory work in Mainz was supported by the German Research Foundation (DFG) through grant GK392 "Composition and Evolution of Crust and Mantle". We are grateful to the staff of the Beijing SHRIMP Center, in particular Jian Ping, for assistance during zircon analyses. We thank the reviewers Karel Schulmann and Peter A. Cawood for suggesting improvements to the manuscript. This is a contribution to IGCP Project 480 and publication no. 388 of the Mainz Geocycles Cluster.

## References

Badarch G, Cunningham WD, Windley BF (2002) A new terrane subdivision for Mongolia: implications for the Phanerozoic crustal growth of Central Asia. J Asian Earth Sci 21:87–110

Bayasgalan A, Jackson J, Ritz JF, Carretier S (1999) 'Forebergs', flowers structures, and the development of large intra-continental strike-slip fault: the Gurvan Bogd fault system in Mongolia. J Struct Geol 21:1285–1302

Berzin NA, Coleman RG, Dobretsov NL, Zonenshain LP, Xuchang X, Chang EZ (1994) Geodynamic map of the western part of the Paleoasian ocean. Russ Geol Geophys 35:5–22

Buchan C, Cunningham D, Windley BF, Tomurhuu D (2001) Structural and lithological characteristics of the Bayankhongor Ophiolite Zone, Central Mongolia. J Geol Soc London 158:445–460

Buchan C, Pfänder J, Kröner A, Brewer TS, Tomurtogoo O, Tomurhuu D, Cunningham D, Windley BF (2002) Timing of accretion and collisional deformation in the Central Asian Orogenic Belt: implications of granite geochronology in the Bayankhongor Ophiolite Zone. Chem Geol 192:23–45

Buslov MM, Saphonova IYu, Watanabe T, Obut OT, Fujiwara Y, Iwata K, Semakov NN, Sugai Y, Smirnova LV, Kazansky AY (2001) Evolution of the Paleo-Asian Ocean (Altai–Sayan Region, Central Asia) and collision of possible Gondwana-derived terranes with the southern marginal part of the Siberian continent. Geos J 5:203–224

Claoué-Long JC, Compston W, Roberts J, Fanning CM (1995) Two Carboniferous ages: a comparison of SHRIMP zircon dating with conventional zircon ages and 40Ar/39Ar analysis. In: Bergen WA, Kent DV, Aubrey MP, Hardenbol J (eds) Geochronology time scales and global stratigraphic correlation. SEPM Special Publication 54:3–20

Corfu F, Hanchar JM, Hoskin PWO, Kinny P (2003) Atlas of zircon textures. In: Hanchar JM, Hoskin PWO (eds) Zircon. Reviews in mineralogy & geochemistry 53:469–500. Mineralogical Society of America, Washington

Cowgill E, Yin A, Harrison TM, Wang XF (2003) Reconstruction of the Altyn Tagh fault based on U–Pb geochronology: role of back thrusts, mantle sutures, and heterogeneous crustal strength in forming the Tibetan Plateau. J Geophys Res 108(B7):2346

Cunningham D (2005) Active intracontinental transpressional mountain building in the Mongolian Altai: defining a new class of orogen. Earth Planet Sci Lett 240:436–444

De Laeter JR, Kennedy AK (1998) A double focusing mass spectrometer for geochronology. Int J Mass Spec 178:43–50

Didenko AN, Mossakovsky AA, Pechersky DM, Ruzhenstev SV, Samygin SG, Kheraskova TN (1994) Geodynamics of the Central-Asian Paleozoic oceans. Russ Geol Geophys 35:59–75

Dijkstra AH, Brouwer FM, Cunningham WD, Buchan C, Badarch G, Mason PRD (2006) Late Neoproterozoic proto-arc ocean crust in the Dariv Range, western Mongolia: a supra-subduction zone end-member ophiolite. J Geol Soc London 163:363–373

Dobretsov NL, Buslov MM (2007) Late Cambrian-Ordovician tectonics and geodynamics of Central Asia. Russ Geol Geophys 48:1–2

Dobretsov NL, Buslov MM, Vernikovsky VA (2003) Neoproterozoic to early Ordovician evolution of the Paleo-Asian ocean: Implications to the break-up of Rodinia. Gond Res 6:143–159

Filippova IB, Bush VA, Didenko AN (2001) Middle Paleozoic subduction belts: the leading factor in the formation of the Central Asian fold-and-thrust belt. Russ J Earth Sci 3:405–426

Frost BR, Barnes CG, Collins WJ, Arculus RJ, Ellis DJ, Frost CD (2001) A geochemical classification for granitic rocks. J Petrol 42:2033–2048

Gehrels GE, Yin A, Wang XF (2003) Magmatic history of the northeastern Tibetan Plateau. J Geophys Res 108(B9):2423

Gladkochub D, Pisarevsky S, Donskaya T, Natapov L, Mazukabzov A, Stanevich A, Sklyarov E (2006) The Siberian Craton and its evolution in terms of the Rodinia hypothesis. Episodes 26:169–174

Hargrove US, Stern RJ, Kimura JI, Manton WI, Johnson P (2006) How juvenile is the Arabian-Nubian Shield? Evidence from Nd isotopes and pre-Neoproterozoic inherited zircons. Earth Planet Sci Lett 252:308–326

Helo C, Hegner E, Kröner A, Badarch G, Tomurtogoo O, Windley BF, Dulski P (2006) Geochemical signature of Paleozoic accretionary complexes of the Central Asian Orogenic Belt in South Mongolia: Constraints on arc environments and crustal growth. Chem Geol 227:236–257

Irvine TN, Baragar WR (1971) A guide to the chemical classification of the common volcanic rocks. Can J Earth Sci 8:523–548

Jahn BM, Wu F, Chen B (2000) Massive granitoid generation in Central Asia; Nd isotope evidence and implication for continental growth in the Phanerozoic. Episodes 23:82–92

Khain EV, Bibikova EV, Salnikova EE, Kröner A, Gibsher AS, Didenko AN, Degtyarev KE, Fedotova AA (2003) The Palaeo-Asian ocean in the Neoproterozoic and early Palaeozoic: new geochronologic data and palaeotectonic reconstructions. Precamb Res 122:329–358

Kheraskova TN, Didenko AN, Bush VA, Volozh YA (2003) The Vendian-Early Paleozoic history of the continental margin of eastern Paleogondwana, Paleoasian Ocean, and Central Asian Foldbelt. Russ J Earth Sci 5:165–184

Kotov AB, Kozakov IK, Bibikova EV, Salnikova EB, Kirnozova TI, Kovach VP (1995) Duration of regional metamorphic episodes in areas of polycyclic endogenic processes: a U–Pb geochronological study. Petrology 3:567–575

Kovach VP, Jian P, Yarmolyuk VV, Kozakov IK, Kovalenko VI, Liu DY, Terent'eva LB (2005) Magmatism and geodynamics of early stages of the Paleoasian ocean formation: geochronological and geochemical data on ophiolites of the Bayan-Khongor zone. Doklady Earth Sci 404:1072–1077

Kovalenko VI, Yarmolyuk VV, Kovach VP, Kotov AB, Kozakov IK, Salnikova EB, Larin AM (2004) Isotope provinces, mechanisms of generation and sources of the continental crust in the Central Asian mobile belt: geological and isotopic evidence. J Asian Earth Sci 23:605–627

Kozakov IK, Kotov AB, Kovach VP, Salnikova EB (1997) Crustal growth in the geologic evolution of the Baidarik Block, Central Mongolia: evidence from Sm–Nd isotopic systematics. Petrology 5:201–207

Kozakov IK, Kotov AB, Salnikova EB, Bibikova EV, Kovach VP, Kirnozova TI, Berezhnaya NG, Lykhin DA (1999) Metamorphic age of crystalline complexes of the Tuva-Mongolia Massif: The U–Pb geochronology of granitoids. Petrology 7:177–191

Kozakov IK, Salnikova EB, Khain EV, Kovach VP, Berezhnaya NG, Yakovleva NG, Plotkina YV (2002) Early Caledonian crystalline rocks of the Lake zone, Mongolia: Stages and tectonic environments as deduced from U–Pb and Sm–Nd isotopic data. Geotectonics 36:156–166

Kozakov IK, Salnikova EB, Natman A, Kovach VP, Kotov AB, Podkovyrov VN, Plotkina YuV (2005) Metasedimentary complexes of the Tuva-Mongolian Massif: Age, provenances, and tectonic position. Strat Geol Corr 13:1–20

Kozakov IK, Salnikova EB, Yakovleva SZ, Plotkina YuV, Fedoseenko AM (2006) Vendian metamorphism in the accretionary-collisional structure of Central Asia. Doklady Earth Sci 407:192–197

Kozakov IK, Salnikova EB, Wang T, Didenko AN, Plotkina YuV, Podkovyrov VN (2007) Early Precambrian crystalline complexes of the Central Asian microcontinent: Age, sources, tectonic position. Strat Geol Corr 15:121–140

Kröner A, Tomurtogoo O, Badarch G, Windley BF, Kozakov IK (2001) New zircon ages and significance for crustal evolution in Mongolia. In: Sklyarov EV (ed) Assembly and break up of Rodinia supercontinent, Irkutsk, 142–145

Kröner A, Windley BF, Badarch G, Tomurtogoo O, Hegner E, Jahn BM, Gruschka S, Khain EV, Demoux A, Wingate MTD (2007) Accretionary growth and crust formation in the Central Asian Orogenic Belt and comparison with the Arabian-Nubian-Shield. Geol Soc Am Mem 200:181–209

Kuzmichev A, Bibikova EV, Zhuravlev DZ (2001) Neoproterozoic (~ 800 Ma) orogeny in the Tuva-Mongolia Massif (Siberia): island arc-continent collision at the northeast Rodinia margin. Precamb Res 110:109–126

Larionov AN, Andreichev VA, Gee DG (2004) The Vendian alkaline igneous suite of northern Timan: ion microprobe U–Pb zircon ages of gabbros and syenite. In: Gee DG, Pease VL (eds) The neoproterozoic timanide orogen of eastern Baltica. Geol Soc London Mem 30:69–74

Lu S, Li H, Zhang Ch, Niu G (2008) Geological and geochronological evidence for the Precambrian evolution of the Tarim craton and surrounding continental fragments. Precamb Res 160:94–107

Ludwig KR (2003) User's Manual for ISOPLOT/Ex 3.0. A geochronological toolkit for microsoft excel. Berkeley Geochronology Center Special Publication 4, pp 70

Mitrofanov FP, Kozakov IK, Palei IP (1981) Precambrian of western Mongolia and southern Tuva. Nauka Publishing House, Leningrad (in Russian)

Mitrofanov FP, Bibikova EV, Gracheva T, Kozakov IK, Sumin LV, Shuleshko IK (1985) Archean isotopic age of grey tonalitic gneisses in Celedonian structures of central Mongolia. Doklady Acad Nauk USSR 284:670–675

Mossakovsky AA, Ruzhentsev SV, Samygin SG, Kheraskova TN (1993) Central Asian fold belt: geodynamic evolution and history of formation. Geotectonics 6:3–33

Nelson DR (1997) Compilation of SHRIMP U–Pb zircon geochronology data. 1996. Geological Survey of Western Australia Record 1997/2, pp 189

Nesbitt HW, Young GM (1982) Early Proterozoic climates and plate motions inferred from major element chemistry of lutites. Nature 299:715–717

Pearce JA, Harris NBW, Tindle AG (1984) Trace element discrimination diagrams for the tectonic interpretation of granitic rocks. J Petrol 25:956–983

Pfänder JA, Kröner A (2004) Tectono-magmatic evolution, age and emplacement of the Agardagh Tes-Chem ophiolite in Tuva, Central Asia: Crustal growth by island arc accretion. In: Kusky T (ed) Precambrian ophiolites and related rocks. Elsevier Science, Amsterdam, pp 207–221

Pisarevsky SA, Natapov LM (2003) Siberia and Rodinia. Tectonophysics 375:221–245

Pisarevsky SA, Natapov LM, Donskaya TV, Gladkochub DP, Vernikovsky VA (2008) Proterozoic Siberia: a promontory of Rodinia. Precamb Res 160:66–76

Rudnick RL, Fountain DM (1995) Nature and composition of the continental crust: a lower crustal perspective. Rev Geophys 33:267–309

Salnikova EB, Kozakov IK, Kotov AB, Kröner A, Todt W, Bibikova EV, Nutman A, Yakopvleva SZ, Kovach VP (2001) Age of Paleozoic granites and metamorphism in the Tuvino-Mongolian Massif of the Central Asian mobile belt: Loss of a Precambrian microcontinent. Precamb Res 110:143–164

Sengör AMC, Natal'in BA, Burtman VS (1993) Evolution of the Altaid tectonic collage and Paleozoic crustal growth in Eurasia. Nature 364:299–307

Shand SJ (1951) Eruptive rocks. 4th edition New York John Wiley, pp 488

Smelov AP, Timofeev AF (2007) The age of the North Asian Cratonic basement: an overview. Gond Res 12:279–288

Sun SS, McDonough WF (1989) Chemical and isotopic systematics of oceanic basalts: implications for mantle composition and

processes. In: Saunders AD, Norry MJ (eds) Magmatism in Ocean Basins. J Geol Soc London Special Publications 42:313–345

Tapponnier P, Molnar P (1979) Active faulting and Cenozoic tectonics of the Tien Shan, Mongolia, and Baykal regions. J Geophys Res 84:3425–3459

Vassallo R, Jolivet M, Ritz JF, Braucher R, Larroque C, Sue C, Todbileg M, Javkhlanbold D (2007) Uplift age and rates of the Gurvan Bogd system (Gobi-Altay) by apatite fission track analysis. Earth Planet Sci Lett 259:333–346

Vernikovsky VA, Vernikovskaya AE, Wingate MTD, Popov NV, Kovach VP (2007) The 880–864 Ma granites of the Yenisey Ridge, western Siberian margin: Geochemistry, SHRIMP geochronology, and tectonic implications. Precamb Res 154:175–191

Wang T, Zheng Y, Gehrels GE, Mu Z (2001) Geochronological evidence for existence of South Mongolian microcontinent; a zircon U–Pb age of granitoid gneisses from the Yagan-Onch Hayrhan metamorphic core complex on the Sino-Mongolian border. Chin Sci Bull 46:2005–2008

Williams IS (1998) U–Th–Pb Geochronology by ion microprobe. In: Applications in micro-analytical techniques to understanding mineralizing processes. Rev Econ Geol 7:1–35

Windley BF, Alexeiev D, Xiao WJ, Kröner A, Badarch G (2007) Tectonic models for accretion of the Central Asian Orogenic Belt. J Geol Soc London 164:31–47

Yarmolyuk VV, Kovalenko VI, Salnikova EB, Kozakov IK, Kotov AB, Kovach VP, Vladykin NV, Yakovleva SZ (2005) U–Pb age of syn- and post-metamorphic granitoids of south Mongolia: evidence for the presence of Grenvillides in the Central Asian Foldbelt. Doklady Earth Sci 404:986–990

Yarmolyuk VV, Kovalenko VI, Kovach VP, Rytsk EY, Kozakov IK, Kotov AB, Salnikova EB (2006) EEarly Stages of the Paleoasian Ocean formation: results of geochronological, isotopic, and geochemical investigations of late Riphean and Vendian-Cambrian complexes in the Central Asian Foldbelt. Doklady Earth Sci 411:1184–1189

Zabotkin LB (1988) Geological Map L47-XXX, 1:200,000. Open file report 4276, Geological Funds of Mongolia, Ulaanbaatar, Mongolia (In Russian)

Zhao Y, Song B, Zhang SH (2006) The Central Mongolian microcontinent: Its Yangtze affinity and tectonic implications. In: Jahn BM, Chung L (eds) Abst.-vol., Symposium on continental growth and orogeny in Asia Taipei Taiwan March 19–26, pp 135–136